Electromechanical study of carbon fiber composites

Xiaojun Wang, Xuli Fu, and D. D. L. Chung
Composite Materials Research Laboratory, State University of New York at Buffalo, Buffalo, New York 14260-4400

(Received 16 June 1997; accepted 30 January 1998)

Electromechanical testing involving simultaneous electrical and mechanical measurements under load was used to study the fiber-matrix interface, the fiber residual compressive stress, and the degree of marcelling (fiber waviness) in carbon fiber composites. The interface study involved single fiber pull-out testing while the fiber-matrix contact electrical resistivity was measured. The residual stress study involved measuring the electrical resistance of a single fiber embedded in the matrix while the fiber was subjected to tension through its exposed ends. The marcelling study involved measuring the electrical resistance of a composite in the through-thickness direction while tension within the elastic regime was applied in the fiber direction.

I. INTRODUCTION

Due to the high strength, high modulus, and low density of carbon fibers, carbon fibers are widely used as a reinforcement in composite materials. Composites utilizing carbon fibers are most commonly polymer-matrix composites, although they include carbon-matrix, cement-matrix, and metal-matrix composites. Applications of these composites include those related to the aerospace, automobile, marine, construction, sporting goods, and biomedical industries.

Due to the technological importance of carbon fiber composites, much fundamental research has been conducted by numerous workers on the structure and properties of these materials. Experimental techniques used for the research include mechanical testing, electrical measurements, fiber-matrix bond testing (by single fiber pull-out or push-in testing, or by single fiber fragmentation testing), microscopy, surface analysis, and thermal analysis. These techniques have their limitations. For example, microscopy and surface analysis give information on the structure of the composite, but do not provide bond strength data; fiber pull-out testing provides bond strength data, but does not give information on the structure of the fiber-matrix interface. Electrical measurements provide information on the structure, since carbon fibers are electrically conducting. However, interpretation of the results in terms of the structure is often complicated by the multiplicity of factors that affect the electrical behavior. For example, both fiber waviness (also called marcelling) and delamination affect the through-thickness resistivity of a continuous carbon fiber polymer-matrix composite laminate. Fiber waviness increases the chance that adjacent fiber layers touch one another, thereby decreasing the through-thickness resistivity. However, delamination increases this resistivity. The decoupling of these factors is difficult or impossible. Mechanical testing provides practical, important data on the mechanical behavior, but interpretation of the results in terms of the structure is also complicated by the multiplicity of factors that affect the mechanical behavior. For example, both marcelling and fiber breakage decrease the tensile strength of a continuous fiber laminate along the fiber direction.

To help alleviate this problem, this paper presents a new method, namely electromechanical testing, for studying the structure and properties of composite materials. This method involves simultaneous electrical and mechanical measurements on the same sample under load, in contrast to the separate electrical and mechanical measurements in previous work.[1,2] This paper illustrates the power of electromechanical testing in studying (i) the fiber-matrix interface (both bond strength and structure aspects), (ii) the fiber residual stress, and (iii) marcelling.

II. FIBER-MATRIX INTERFACE

The fiber-matrix interface is critical to the properties of composite materials. A sufficiently strong interface is needed in order for load transfer to the fibers to occur. The bond strength and interfacial structure are closely related. The desirable interfacial phase depends on the origin of bonding, but, interfacial voids are in general undesirable. Increase of the bond strength requires appropriate change of the interfacial structure.

The bond strength is most commonly determined under shear by single fiber pull-out testing, in which a single fiber is embedded at one end in the matrix and then pulled out from the free end. This technique does not provide information on the interfacial structure. It also suffers from the large scatter in data for interfaces that are identically prepared. The scatter stems from the variation in the interface cleanliness among samples that are identically prepared, as fiber-matrix interface samples are typically prepared without vacuum, clean room, or other clean environments, and contamination tends to be

present on the fiber surface or in the matrix (particularly if the matrix is cement).

This problem can be alleviated by measuring both bond strength and contact electrical resistivity for each interface sample and seeing how these two quantities correlate among samples that are identically prepared. The sense of the correlation provides information on the origin of bonding. For example, decrease of the contact resistivity with increasing bond strength means that interfacial voids govern the bond strength; a higher void content causes the contact resistivity to increase and causes the bond strength to decrease. On the other hand, increase of the contact resistivity with increasing bond strength means that an interfacial phase of high volume resistivity helps the bonding; the more abundant is this phase, the higher is the contact resistivity and the greater is the bond strength. A change in the interfacial structure, as caused by surface treatment of the fiber or by change in composition of the matrix, causes the curve of contact resistivity versus bond strength to shift. By observing the shift in the curve, even a small change in the bond strength resulting from the change in the interfacial structure can be discerned. This technique, called electromechanical pull-out testing,[3] is illustrated below for the interface between carbon fiber and cement matrix.

The interface between carbon fiber and cement matrix is relevant to carbon fiber reinforced concrete, which is technologically attractive due to its low drying shrinkage, high flexural strength and toughness, and self-sensing ability.[4–11]

A. Experimental methods

The carbon fibers were isotropic pitch based and unsized, as obtained from Ashland Petroleum Co. (Ashland, Kentucky). The fiber properties are shown in Table I. As-received and five types of surface treated fibers were used. The surface treatments included immersion (with stirring) of the fibers at room temperature for 24 h in acetic acid (99.9% reagent, 2 N), H_2O_2 (31.2% reagent, 2 N), NaOH solution (98.4% reagent, 1.5 N), or nitric acid (60% reagent, 1.5 N) followed by water washing at room temperature and air drying at 110 °C) and exposure of the fibers to O_3 gas (0.3 vol %, in air) for 10 min at 160 °C. Prior to O_3 exposure, the fibers had been dried at 110 °C in air for 1 h.

TABLE I. Properties of carbon fibers.

Filament diameter	15 ± 3 μm
Tensile strength	690 MPa
Tensile modulus	48 GPa
Elongation at break	1.4%
Electrical resistivity	3.0×10^{-3} Ω cm
Specific gravity	1.6 g/cm^3
Carbon content	98 wt. %

Cement paste made from portland cement (Type 1) from Lafarge Corp. (Southfield, MI) was used for the cementitious material. Three types of pastes were used, namely (i) plain cement paste (with only cement and water, such that the water-cement ratio is 0.45), (ii) cement paste with methylcellulose in the amount of 0.4% by weight of cement (together with water reducing agent in the amount of 1% by weight of cement, and with water-cement ratio = 0.32), and (iii) cement paste with latex in the amount of 20% by weight of cement (water-cement-ratio = 0.23, without water-reducing agent). The water-reducing agent used in cement paste (ii) was TAMOL SN (Rohm and Haas Co., Philadelphia, PA), which contained 93–96% sodium salt of a condensed naphthalenesulfonic acid. Methylcellulose (Dow Chemical, Midland, MI, Methocel A15-LV) in the amount of 0.4% of the cement weight was used in paste (ii). The defoamer (Colloids Inc., Marietta, GA, 1010) used whenever methylcellulose was used was in the amount of 0.13 vol %. The latex (Dow Chemical, Midland, MI, 460NA) used in cement paste (iii) was a styrene-butadiene polymer; it was used in the amount of 20% of the weight of the cement. The antifoam (Dow Corning, Midland, MI, 2210) used whenever latex was used was in the amount of 0.5% of the weight of the latex.

A Hobart mixer with a flat beater was used for mixing. For the case of cement paste containing latex, the latex and antifoam first were mixed by hand for about 1 min. Then this mixture, cement, water, and the water reducing agent were mixed in the mixer for 5 min. For the case of cement paste containing methylcellulose, methylcellulose was dissolved in water and then the defoamer was added and stirred by hand for about 2 min. Then this mixture, cement, water, and water reducing agent were mixed in the mixer for 5 min.

The contact electrical resistivity between the fiber and the cement paste was measured at 28 days of curing using the four-probe method (method involving four probes, the outer two for passing current and the inner two for measuring the voltage) and silver paint as electrical contacts, as illustrated in Fig. 1. One current contact and one voltage contact were on the fiber, while the other voltage and current contacts were on the cement paste embedding the fiber to a distance ranging from 0.51 to 1.20 mm, as measured for each specimen. The cement paste thickness was 1 mm on each side, sandwiching the fiber. The fiber length was 1 cm. The resistance between the two voltage probes was measured by using a Keithley 2001 multimeter; it corresponds to the sum of the fiber volume resistance, the interface contact resistance, and the cement paste volume resistance; the current-voltage relationship was linear. The measured resistance turned out to be dominated by the contact resistance, to the extent that the two volume resistance terms can be neglected. The contact resistivity (in $\Omega \cdot \text{cm}^2$) is given

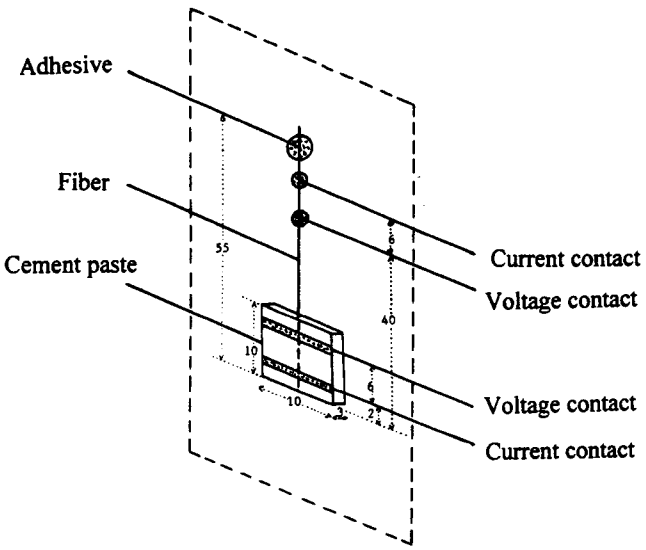

FIG. 1. Sample configuration for measuring the contact electrical resistivity of the interface between a fiber and cement paste during pull-out testing. Dimensions shown are in mm.

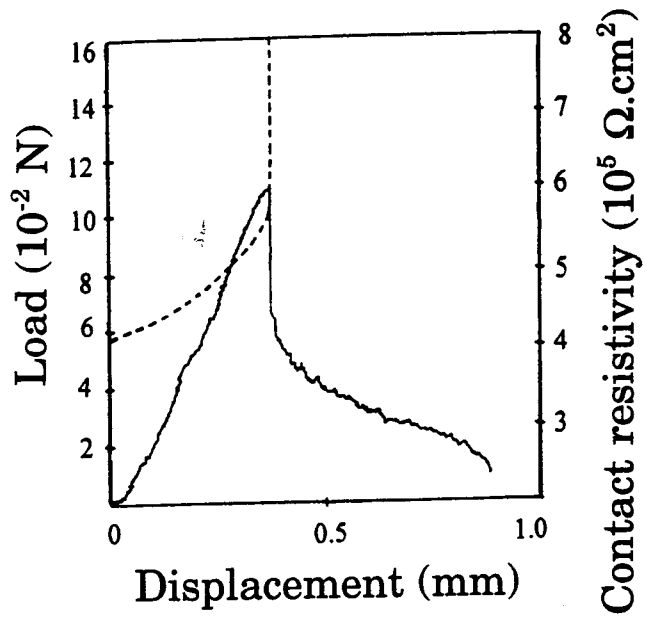

FIG. 2. Plots of load versus displacement (solid curve) and of contact electrical resistivity versus displacement (dashed curve) simultaneously obtained during pull-out testing of carbon fiber from cement paste at 28 days of curing.

by the product of the contact resistance (in Ω) and the contact (interface) area (in cm^2), such that the contact area depends on the embedment length of the particular specimen.

Single fiber pull-out testing was conducted on the same interface samples and at the same time as the contact resistivity was measured. For pull-out testing, one end of the fiber was embedded in cement paste, as in Fig. 1. A Sintech 2/D screw-action mechanical testing system was used. The contact resistivity was taken as the value prior to pull-out testing. The shear bond strength was taken as the maximum load during pull-out testing divided by the surface area of the embedded part of the fiber. Figure 2 gives typical plots of load versus displacement and of contact resistivity versus displacement simultaneously obtained during pull-out testing.

The dynamic contact angle between carbon fiber and de-ionized water was measured using the Sigma 70 tensiometer of KSV Instruments (Monroe, CT). The tensiometric method (micro-Wilhemy technique) was used.[12] The immersion depth was up to 3 mm and the stage with a beaker of water was moved up (advancing) and down (receding) at a constant speed of 3 mm/min. Five samples of each type were tested.

B. Results and discussion

Figure 3 shows the correlation of the contact resistivity and the bond strength for plain cement paste in contact with six different types of fibers (as-received and five types of treated fibers, with seven interface samples for each of six fiber types). Among the seven samples (identically prepared, but different in bond strength and contact resistivity due to differences in interface cleanliness) in each case, a high bond strength is associated with a low contact resistivity, because a high bond strength is associated with a low content of interfacial voids, which are electrically insulating. Comparison among the curves in Fig. 3 shows that all treatments increased the contact resistivity and possibly the bond strength as well, such that the magnitude of either effect increased in the order: acetic acid, H_2O_2, NaOH, nitric acid, and O_3. The effect on the bond strength is quite clear for the O_3 case, but less clear for the other treatments. Both effects are mainly attributed to the formation of an interfacial layer of high volume resistivity due to the treatment. This interlayer is shown below (next paragraph) by using ESCA for the O_3 case. It enhances the bonding and increases the contact resistivity. For the oxidizing chemicals, such as acetic acid, H_2O_2, nitric acid, and O_3, the interfacial layer is believed to be oxygen-containing functional groups,[12] which help the wettability of the fibers by the cement.

The advancing and receding contact angles for the first three cycles of advancing (increasing immersion depth) and receding (decreasing immersion depth) are shown in Table II for each of the as-received and NaOH, HNO_3, and O_3 treated fibers. The receding angle was decreased to zero by any of these three treatments. The advancing angle was decreased to zero only for the ozone treated fiber, though it was still substantially decreased for the NaOH and HNO_3 treated fibers. The advancing angle decreased in the order (i) as-received, (ii) NaOH treated, (iii) HNO_3 treated, and (iv) O_3 treated fibers. The

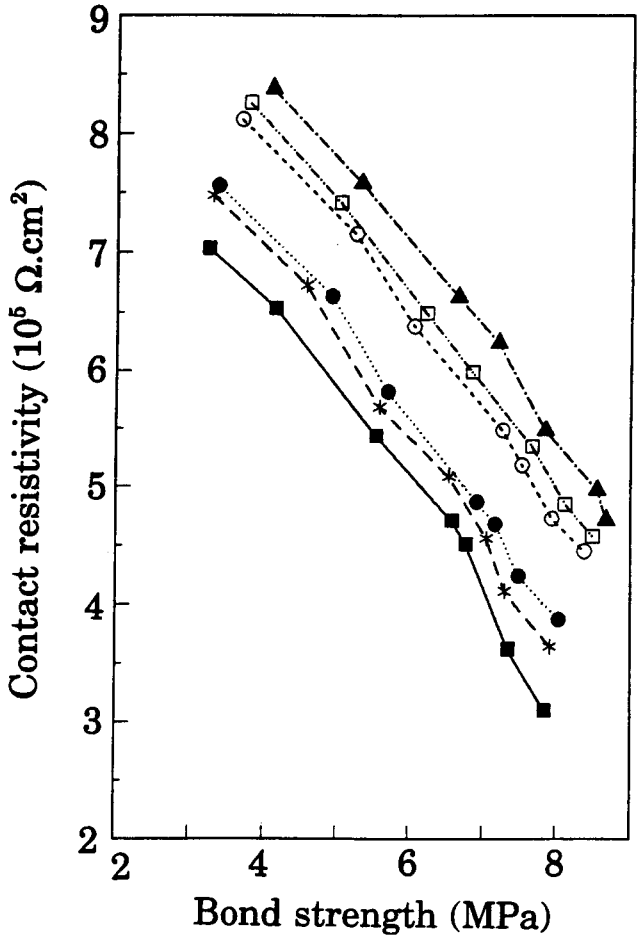

FIG. 3. Variation of contact electrical resistivity with bond strength for plain cement in contact with as-received (●) and five types of treated carbon fibers: acetic acid (*), H_2O_2 (■), NaOH (○), nitric acid (□), and O_3 (▲).

improved wetting is due to the increase in the surface oxygen concentration and change in surface oxygen from C–O to C=O, as shown by the O_{1s} and C_{1s} peaks in ESCA for the case of O_3 treatment (Table III). As cement paste is a hydraulic mix, the improved wetting of the fiber by water means improved wetting of the fiber by the cement paste.

Among the chemicals used, ozone (O_3) is the most oxidizing chemical and nitric acid is the second most oxidizing chemical, so O_3 gave the largest effects while nitric acid gave the second largest effects. The NaOH treatment probably resulted in OH functional groups, which help wettability of the fibers by the cement. Other than increasing the oxygen-containing functional groups, the oxidizing treatments are also believed to increase the active specific surface area,[13] the number of bonding sites on the fiber surface,[14] and the surface roughness.[14] These effects of the treatments also cause bond strength increases, but may not cause contact resistivity increases.

Figure 4 shows the effect of polymer admixtures (methylcellulose and latex) on the bond between as-received carbon fibers and cement. Either admixture increased both bond strength and contact resistivity. These effects are due to the polymer admixtures, and are not due to the differences in water-cement ratio. The water-cement ratio decreased in the order: cement pastes (i), (ii), and (iii). In a separate study of the effect of the water-cement ratio (no polymer admixture), two of the authors (Fu and Chung) found that the bond strength decreases and the contact resistivity slightly increases with decreasing water-cement ratio, due to the decrease in fluidity of the mix and the consequent increase in interfacial void content as the water-cement ratio decreases.[15] As shown in Fig. 4, the polymer admixtures increased the bond strength, in spite of the low water-cement ratio in cement pastes with polymer admixtures [i.e., pastes (ii) and (iii)]. The increase in contact resistivity is because the polymers are less conducting than cement. The increase in bond strength is because the polymers improve the adhesion between fiber and cement. Latex gave larger effects than methylcellulose, at least partly because latex was present in a much larger quantity than methylcellulose. Also shown in Fig. 4 are the data (also in Fig. 3) for plain cement in contact with O_3 treated fibers. The O_3 treatment of the fibers was even more effective than the use of polymer admixtures for enhancing the bond strength.

Although the increase in bond strength due to ozone treatment was slight (Fig. 3), the bond strength increase

TABLE II. The contact angle (degrees, ±1) between carbon fiber and water.

Fiber		Advancing	Receding
As-received	1st cycle	86.1	30.2
	2nd cycle	84.9	28.5
	3rd cycle	83.2	28.3
	Average	84.7	29.0
NaOH treated	1st cycle	40.6	0
	2nd cycle	38.8	0
	3rd cycle	37.6	0
	Average	39.0	0
HNO_3 treated	1st cycle	35.1	0
	2nd cycle	32.5	0
	3rd cycle	28.4	0
	Average	32.0	0
O_3 treated	1st cycle	0	0
	2nd cycle	0	0
	3rd cycle	0	0
	Average	0	0

TABLE III. Fractions of surface carbon atoms bonded as C–H, C–O, and C=O.

	C–H	C–O	C=O
As-received	86.5%	13.5%	0
After O_3 exposure	76.0%	0	24.0%

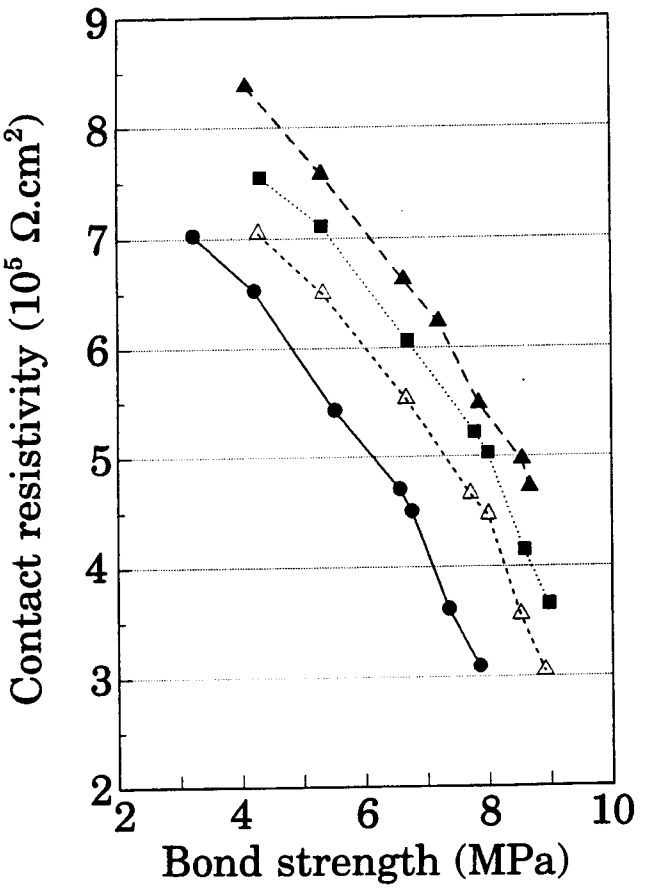

FIG. 4. Variation of contact electrical resistivity with bond strength for as-received carbon fibers in contact with plain cement (●), cement with methylcellulose (△), and cement with latex (■). Also shown is that for O_3 treated fiber in contact with plain cement (▲).

caused substantial increases in tensile strength, modulus, and ductility of cement paste containing carbon fibers.[16]

C. Summary

The bond strength between carbon fiber and cement was slightly enhanced by oxidizing treatments, such as ozone and nitric acid treatments, mainly due to the resulting increase in surface oxygen concentration and change in surface oxygen from C–O to C=O (at least for the ozone treatment) helping the wettability of the fibers by the cement. The highest bond strength was attained by ozone treatment. The increase in bond strength was associated with an increase in the fiber-cement contact resistivity due to the high resistivity of the oxygen-containing functional groups. The bond strength and contact resistivity were also enhanced by polymer admixtures in the cement mix. Latex gave larger effects than methylcellulose, but less effect than ozone treatment of the fibers.

The technique described in this section is limited to matrices that are at least a little conducting electrically.

III. FIBER RESIDUAL STRESS

Due to the shrinkage of the matrix during composite fabrication and/or the thermal contraction mismatch between fiber and matrix during cooling near the end of composite fabrication, the fibers in a composite can have a residual compressive stress.[17–20] This stress may affect the structure of the fiber so that the fiber properties are affected, often adversely.

The measurement of the fiber residual strain by x-ray diffraction, Raman scattering, and other optical techniques is difficult due to the anisotropy of the fiber strain and the necessity of embedding the fiber in the matrix. Electromechanical testing provides a simple and effective method for measuring the fiber residual stress along the fiber direction, as illustrated below for the case of carbon fiber in epoxy. Carbon fiber epoxy-matrix composites are the most widely used form of carbon fiber composites due to the good adhesion between fiber and epoxy.

It is known that the disparate thermal expansion properties of carbon fiber and epoxy leads to an inevitable buildup of residual thermal stress during the matrix (epoxy) solidification and subsequent cooling. Here we consider only the residual stress along the fiber direction (one dimension). Since the strain of matrix and fiber is the same (if adhesion is perfect),

$$\frac{\sigma_f}{E_f} + \alpha_f \Delta T = \frac{\sigma_m}{E_m} + \alpha_m \Delta T , \qquad (1)$$

where σ_f is the longitudinal residual stress built up in the fiber, σ_m is the residual stress built up in the matrix, E_f is the modulus of fiber, E_m is the modulus of matrix, α_f is the coefficient of thermal expansion of fiber, α_m is the coefficient of thermal expansion of matrix, and ΔT is the temperature change. Since there is no external force on the specimen,

$$\sigma_f V_f + \sigma_m V_m = 0 , \qquad (2)$$

where V_f is the volume fraction of fiber and V_m is the volume fraction of matrix.

Combining Eqs. (1) and (2), we have the following equation for calculating the residual stress in the fiber:

$$\sigma_f = \frac{E_f E_m V_m (\alpha_m - \alpha_f) \Delta T}{(V_m E_m + V_f E_f)} . \qquad (3)$$

In this work, $E_f = 221$ GPa, $E_m = 3.7$ GPa, $\alpha_m = 42 \times 10^{-6}$ K^{-1}, $\alpha_f = 0.09 \times 10^{-6}$ K^{-1}, and $\Delta T = 155$ K. From Eq. (3), the residual thermal stress built up in the fiber reaches 1438 MPa.

A. Experimental methods

The carbon fiber used was 10E-Torayca T-300 (unsized, PAN-based), of diameter 7 μm, density 1.76 g/cm^3, tensile modulus 221 ± 4 GPa, tensile

strength 3.1 ± 0.2 GPa, and ultimate elongation 1.4%. The electrical resistivity was (2.2 ± 0.5) × 10^{-3} Ω · cm, as measured by using the four-probe method and silver paint electrical contacts on single fibers. The epoxy used was EPON(R) resin 9405 together with curing agent 9470, both from Shell Chemical Co., in weight ratio 70:30. The recommended curing temperature is 150–180 °C for this epoxy.

The electrical resistance of a carbon fiber embedded in epoxy before and after the curing of the epoxy (at 180 °C, without pressure, for 2 h), as well as during subsequent tensile loading, was measured using the sample configuration of Fig. 5. A single fiber was embedded in epoxy for a length of 60 mm and an epoxy coating thickness of 5 mm, such that both ends of the fiber protruded and were bare in order to allow electrical contacts to be made on the fiber using silver paint. Four contacts (labeled A, B, C, and D in Fig. 5) were made. The outer two contacts (A and D) were for passing a current, whereas the inner two contacts (B and C, 80 mm apart) were for measuring the voltage. A Keithley 2001 multimeter was used for dc electrical measurements.

Table IV shows the electrical resistivity of carbon fiber before curing of epoxy and after both curing and subsequent cooling. Data for six samples are consistent, indicating that the resistivity of the fiber increased by ~10% after curing and subsequent cooling. The fractional resistance increase was also ~10%. For single fiber in epoxy, residual stress is built up during curing and subsequent cooling. The observed resistance increase after curing and cooling is attributed to this residual stress, which is compressive in the fiber and probably causes a microstructural change in the fiber. However, the type of microstructural change has not been investigated.

TABLE IV. Electrical resistivity of carbon fiber before and after epoxy curing.

Resistivity before curing (10^{-3} Ω · cm)	Resistivity after curing (10^{-3} Ω · cm)	Fractional change in resistivity
2.24	2.46	9.8%
2.43	2.69	10.5%
2.17	2.39	10.2%
2.11	2.34	11.0%
2.58	2.83	9.6%
2.36	2.61	10.7%

Electromechanical testing of a single fiber in cured epoxy was conducted using the configuration of Fig. 5 during tension under load control, as provided by a screw-type mechanical testing system (Sintech 2/D). The crosshead speed was 0.1 mm/min. The strain was obtained from the crosshead displacement.

Figure 6 shows the fractional change in resistance ($\Delta R/R_0$) of fiber in cured epoxy upon static tension up to fiber fracture. Due to the small strains involved, $\Delta R/R_0$ was essentially equal to the fractional change in resistivity. The $\Delta R/R_0$ decreased by up to ~10% upon tension to a strain of ~0.5% (a stress of 1320 MPa) and then increased upon further tension. The magnitude of resistance decrease of carbon fiber in initial tension is close to the value of the prior resistance increase during curing and cooling of epoxy. The stress at which the resistance decrease was complete (1320 MPa) is close to the value of 1438 MPa obtained from Eq. (3). Therefore, the initial decrease in $\Delta R/R_0$ in Fig. 6 is attributed to the reduction of the residual compressive stress in the fiber. The later increase in $\Delta R/R_0$ in Fig. 6 is attributed to damage in the fiber. Previous work on the electromechanical behavior of a bare carbon fiber

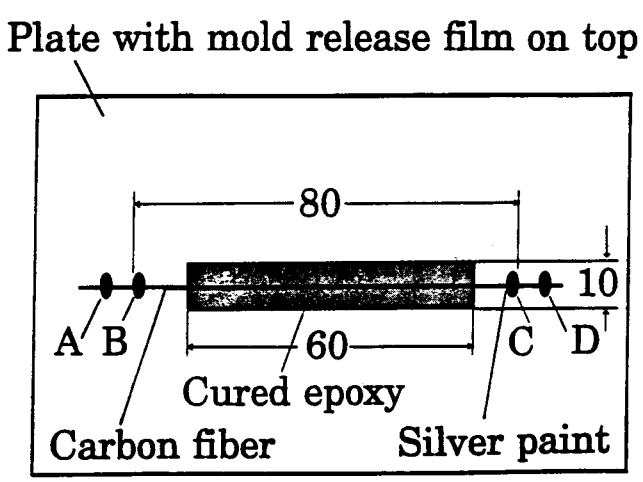

FIG. 5. Sketch of the resistance measurement setup for single carbon fiber embedded in epoxy. A, B, C, and D are four probes. A and D are for passing current; B and C are for voltage measurement. Dimensions are in mm.

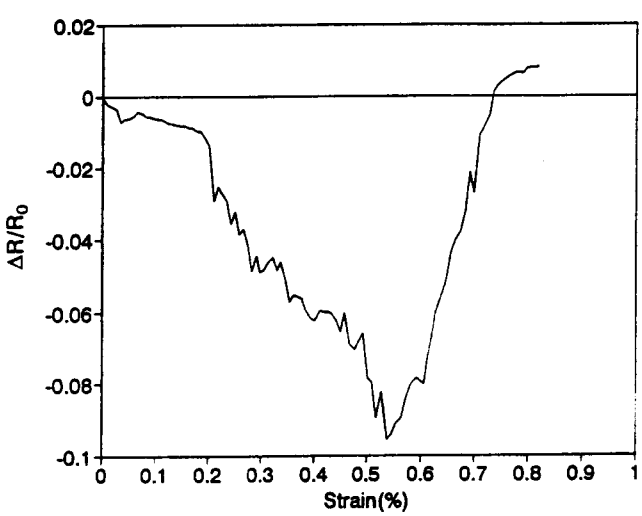

FIG. 6. The fractional electrical resistance change of single carbon fiber in epoxy under tension.

has shown that damage causes the resistivity of the fiber to increase.[21]

Figure 7 shows the $\Delta R/R_0$ of fiber in cured epoxy upon tensile loading to a strain of ~0.3% and upon subsequent unloading. The $\Delta R/R_0$ decreased upon loading and increased back to the initial value upon unloading, indicating the reversibility of the electromechanical effect.

The $\Delta R/R_0$ per unit strain for the electromechanical effect of Fig. 7 is -17 (negative since $\Delta R/R_0$ is negative). In contrast, $\Delta R/R_0$ per unit strain for the electromechanical effect associated with a bare carbon fiber and due to dimensional changes is 2 (positive since $\Delta R/R_0$ is positive).

B. Summary

In summary, a new piezoresistive effect in which the resistivity of a carbon fiber embedded in epoxy decreases reversibly upon tension of the fiber is attributed to the reduction of the residual compressive stress in the fiber. This effect provides a method for measuring the residual stress along the fiber direction. The value thus obtained for carbon fiber in epoxy is 1320 MPa. The residual stress is due to the shrinkage of the epoxy during curing and during subsequent cooling. The effect is opposite to that of the corresponding bare carbon fiber (tested electromechanically using the same method as in this work), which reversibly increases in resistance (not resistivity) upon tension due to dimensional changes.[21]

The technique described in this section is most suitable for matrices that are electrically insulating. Data interpretation will be complicated by a matrix that is a little conducting, even if it is less conducting than the fiber.

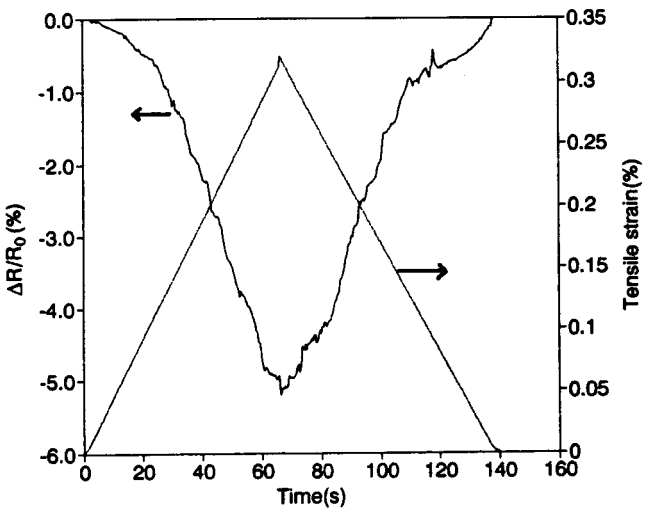

FIG. 7. Plots of $\Delta R/R_0$ versus time and strain versus time during tensile loading and unloading for single carbon fiber embedded in epoxy. Solid curve: $\Delta R/R_0$ versus time. Dashed curve: tensile strain versus time.

IV. MARCELLING

Marcelling (fiber waviness) is a common cause of failure in composite parts, because the marcels can cause localized redistribution of stresses.[2,22] Marcelling to various degrees is inherent in composites, as it is formed during the manufacture of the composites. In order to alleviate this problem, detection of marcelling after the manufacture of a composite is necessary. The use of microscopy to detect marcelling is difficult, especially if the marcelling does not occur at the edge of a composite laminate. Moreover, it is tedious and insensitive to small degrees of waviness. Marcelling affects both mechanical and electrical properties of the composite, but these effects cannot be used to indicate the degree of marcelling, because other structural aspects (such as fiber breakage and delamination) also affect these properties.

Electromechanical testing provides a new and effective method of detecting the degree of marcelling. This technique involves applying tension (within the elastic regime) to the composite panel in the direction of the fibers whose waviness is to be determined (for example, 0° fibers) and simultaneously measuring the electrical resistance of the panel in the through-thickness direction. This procedure is performed during tensile loading and unloading. Due to inherent marcelling, the fibers along the stress axis become less wavy as the tension is applied. Consequently, the chance that adjacent fiber layers touch one another is decreased and the electrical resistivity (dc) of the composite perpendicular to the fiber layers increases. The more severe is the inherent marcelling in the composite, the more is the fractional increase in through-thickness resistance per unit strain in the stress direction. Upon subsequent unloading, the resistance returns to its original value and the strain returns to zero, as this electromechanical phenomenon is reversible.

Delamination as well as reduced marcelling cause increase in the through-thickness resistance. Therefore, electrical measurement (in contrast to electromechanical testing) is not effective for marcel detection. On the other hand, delamination cannot cause an electromechanical effect, whereas marcelling can.

The electromechanical method of marcel detection is illustrated below for the case of a unidirectional continuous carbon fiber epoxy-matrix composite.

A. Experimental methods

Composite samples were constructed from individual layers cut from a 12 in. (30.5 cm) wide unidirectional carbon fiber prepreg tape manufactured by ICI Fiberite (Tempe, AZ). The product used was Hy-E 1076E, which consisted of a 976 epoxy matrix and 10E carbon fibers. The fiber and matrix properties are shown in Table V.

TABLE V. Properties of carbon fiber and epoxy matrix (according to ICI Fiberite) used for continuous carbon fiber composite.

10E - Torayca T-300 (6K) untwisted, UC-309 sized	
Density	1.76 g/cm^3
Tensile modulus	221 GPa
Tensile strength	3.1 GPa
976 Epoxy	
Process temperature	350 °F (177 °C)
Maximum service temperature	350 °F (177 °C) dry 250 °F (121 °C) wet
Flexural modulus	3.7 GPa
Flexural strength	138 MPa
T_g	232 °C
Density	1.28 g/cm^3

The composite laminates were laid up in a 4 × 7 in. (10.2 × 17.8 cm) platten compression mold with laminate configuration $[0]_{14}$. The individual 4 × 7 in. fiber layers (14 per laminate) were cut from the prepreg tape. The layers were stacked in the mold with a mold release film on the top and bottom of the layup. No liquid mold release was used. The laminates were cured using a cycle based on the ICI Fiberite C-5 cure cycle. The curing occurred at 355 ± 10 °F (179 ± 6 °C) and 89 psi (0.61 MPa) for 120 min. Afterward, the laminates were cut to pieces of size 160 × 14 mm. The density and nominal thickness of the laminate were 1.52 ± 0.01 g/cm^3 and 1.4 mm, respectively, after curing. The exact thickness of each specimen cut from the laminate was separately measured in order to determine the longitudinal and transverse resistivities and the longitudinal modulus of the specimen. The volume fraction of carbon fibers in the composite was 58%. Glass fiber reinforced epoxy end tabs were applied to both ends on both sides of each cured piece, such that each tab was 30 mm long and the inner edges of the end tabs on the same side were 100 mm apart and the outer edges were 160 mm apart.

The volume electrical resistance R was measured using the four-probe method while cyclic tension was applied in the longitudinal direction (parallel to fibers). Silver paint was used for all electrical contacts. The four probes consisted of two outer current probes and two inner voltage probes. The resistance R refers to the sample resistance between the inner probes. The longitudinal and through-thickness R were measured in different samples. For the longitudinal R measurement, the four electrical contacts were around the whole perimeter of the sample in four parallel planes that were perpendicular to the stress axis, such that the inner probes were 60 mm apart and the outer probes were 78 mm apart. For the through-thickness R measurement, the current contacts were centered on the largest opposite faces and in the form of open rectangles of length 70 mm in the longitudinal direction, while each of the two voltage contacts was in the form of a solid rectangle (of length 20 mm in the longitudinal direction) surrounded by a current contact (open rectangle). Thus, each face had a current contact surrounding a voltage contact. A strain gage was attached to the very center of one of the largest opposite faces, for both longitudinal and through-thickness R measurement samples. In the case of the through-thickness R measurement sample, the strain gage was at the center of the inner rectangle (voltage contact). A Keithley 2001 multimeter was used. A hydraulic mechanical testing system (MTS 810) was used in the test to provide a displacement rate of 1.0 mm/min.

B. Results

Figure 8 shows the longitudinal stress, strain, and fractional longitudinal resistance increase (longitudinal $\Delta R/R_0$) obtained simultaneously during cyclic tension

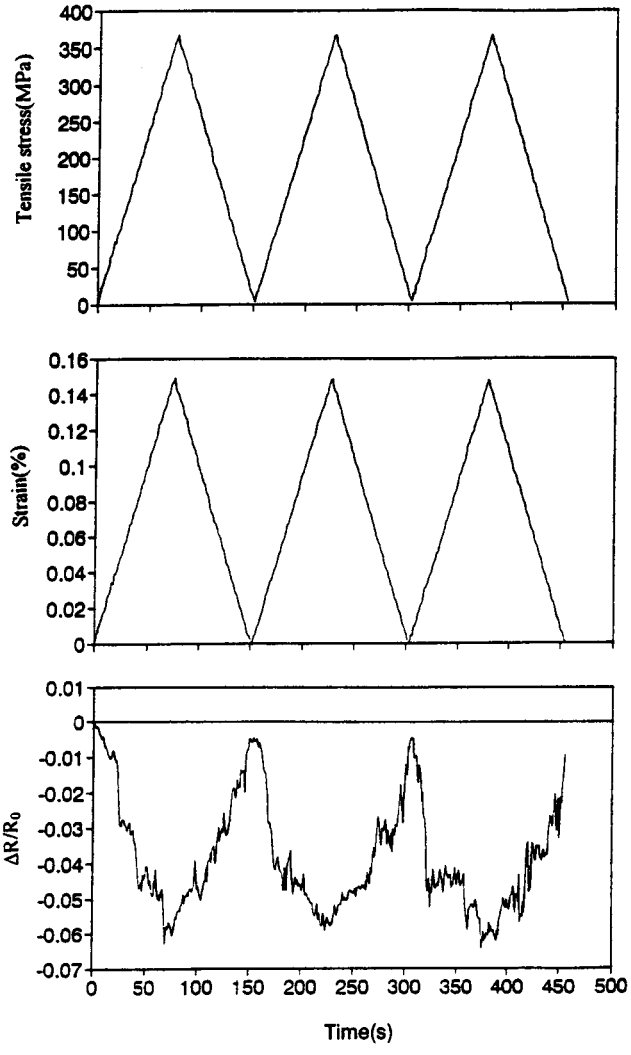

FIG. 8. Longitudinal stress and strain and fractional resistance increase ($\Delta R/R_0$) obtained simultaneously during cyclic tension to a stress amplitude equal to 32% of the breaking stress for continuous carbon fiber epoxy-matrix composite.

to a stress amplitude equal to 32% of the breaking stress. The strain returned to zero at the end of each cycle. Because of the small strains involved, $\Delta R/R_0$ is essentially equal to the fractional increase in resistivity. The longitudinal $\Delta R/R_0$ decreased upon loading and increased upon unloading in every cycle, such that R irreversibly decreased slightly after the first cycle (i.e., $\Delta R/R_0$ did not return to 0 at the end of the first cycle). When the stress amplitude was raised to 36% of the breaking stress, the effect was similar, except that both the reversible and irreversible parts of $\Delta R/R_0$ were larger, as shown in Table VI.

Figure 9 shows the longitudinal stress, strain, and $\Delta R/R_0$ obtained simultaneously during static tensile loading up to fracture. The longitudinal $\Delta R/R_0$ first decreased and then increased in steps as the strain increased. The decrease in $\Delta R/R_0$ in the low strain regime is consistent with the trend in Fig. 8. The difference in the $\Delta R/R_0$ value at the same strain between Figs. 8 and 9 is due to the variation in the degree of marcelling from sample to sample within the same laminate. This variation is addressed later in this paper.

Figure 10 shows the longitudinal stress and strain and the through-thickness $\Delta R/R_0$ obtained simultaneously during cyclic tension to a stress amplitude equal to 35% of the breaking stress. As expected, the strain returned to zero at the end of each cycle. The through-thickness $\Delta R/R_0$ increased upon loading and decreased upon unloading in every cycle, such that R irreversibly decreased slightly after the first cycle (i.e., $\Delta R/R_0$ did not return to 0 at the end of the first cycle). Upon increasing the stress amplitude to 45% of the breaking stress, the effect was similar, except that the reversible part of $\Delta R/R_0$ was larger, as shown in Table VI.

Figure 11 shows the longitudinal stress and strain and through-thickness $\Delta R/R_0$ obtained simultaneously during static tensile loading up to fracture. The through-thickness $\Delta R/R_0$ first increased abruptly and then leveled off as the strain increased.

The tensile modulus was determined from the slope of the stress-strain curve in the elastic regime, as in the regimes in Figs. 8 and 10, for each sample that was tested electromechanically. Figure 12 shows that the absolute value of the reversible part of $\Delta R/R_0$ (both longitudinal and through-thickness) decreases with increasing tensile modulus. In other words, different samples were slightly different in the degree of marcelling, even though they were cut from the same laminate. Nevertheless, a sample with a larger absolute value of the reversible part of $\Delta R/R_0$ tended to have a smaller tensile modulus.

The electrical resistivity in the longitudinal and through-thickness directions under no load is shown in Figs. 13 and 14, respectively. Also shown in Figs. 13 and 14 is the absolute value of the reversible part of $\Delta R/R_0$ in the corresponding direction for each corresponding sample tested electromechanically. The absolute value of the reversible part of the longitudinal $\Delta R/R_0$ increases with increasing longitudinal resistivity (Fig. 13), whereas the reversible part of the through-thickness $\Delta R/R_0$ decreases with increasing through-thickness resistivity (Fig. 14).

C. Discussion

A dimensional change without any resistivity change would have caused R to increase during tensile loading. In contrast, R was observed to decrease (not increase) upon tensile loading. Furthermore, the observed magnitude of $\Delta R/R_0$ was from 9 to 14 times that of $\Delta R/R_0$ calculated by assuming that $\Delta R/R_0$ was due only to dimensional change and not due to any resistivity change. Hence the contribution of $\Delta R/R_0$ from the dimensional change is negligible compared to that from the resistivity change.

The decrease in longitudinal $\Delta R/R_0$ and increase in through-thickness $\Delta R/R_0$ upon longitudinal tension, as observed in this work for a continuous carbon fiber composite in cyclic loading (Figs. 8 and 10) or static loading at low strains (Figs. 9 and 11) are all attributed to the decrease in the degree of marcelling upon longitudinal tension. The decrease in the degree of marcelling causes the longitudinal resistivity to decrease. In addition, it causes the adjacent fiber layers to have less chance of touching one another, so the through-thickness resistivity increases. The effects are almost

TABLE VI. Reversible and irreversible parts of $\Delta R/R_0$ and strain sensitivity in both longitudinal and through-thickness directions at various stress amplitudes for continuous carbon fiber polymer-matrix composite.

		$\Delta R/R_0$		
	Maximum stress/Fracture stress	Reversible	Irreversible	Strain sensitivity[a]
Longitudinal	32%	−0.050	−0.005	−35.7
	36%	−0.068	−0.012	−37.6
Through-thickness	35%	0.06	−0.017	34.2
	45%	0.11	−0.018	48.7

[a]Reversible $\Delta R/R_0$ divided by the longitudinal strain amplitude.

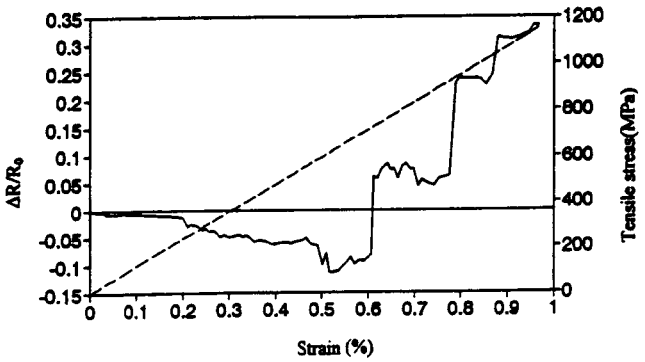

FIG. 9. Longitudinal stress and strain and fractional resistance increase ($\Delta R/R_0$) obtained simultaneously during static tension up to fracture, which occurs at the highest strain in the curves. Solid curve: $\Delta R/R_0$ versus strain. Dashed curve: tensile stress versus strain for continuous carbon fiber epoxy-matrix composite.

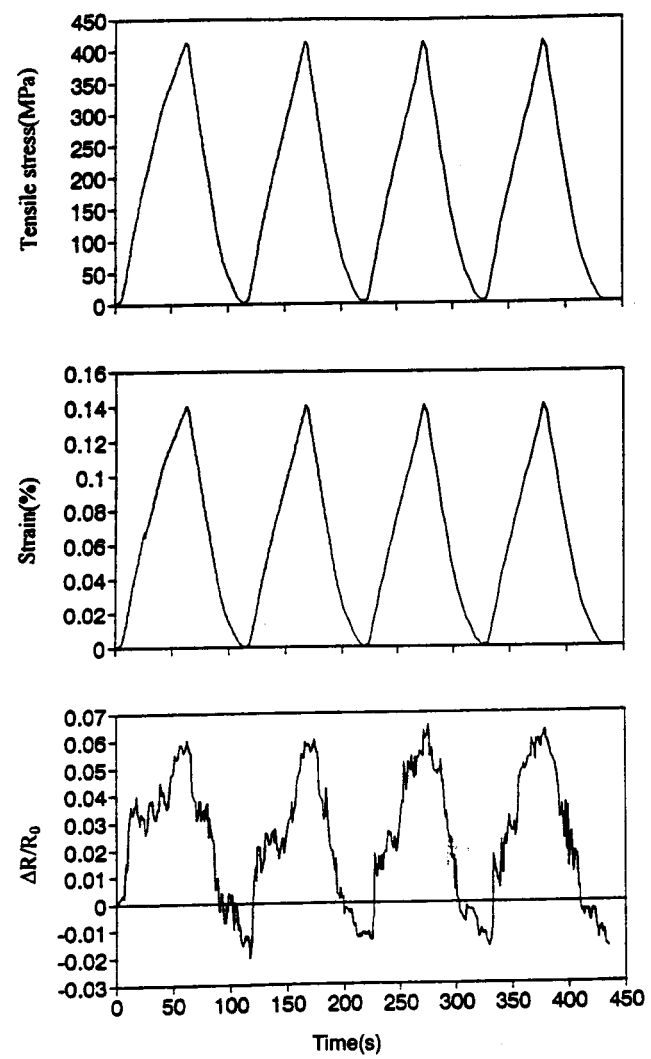

FIG. 10. Longitudinal stress and strain and the through-thickness $\Delta R/R_0$ obtained simultaneously during cyclic tension to a stress amplitude equal to 35% of the breaking stress for continuous carbon fiber epoxy-matrix composite.

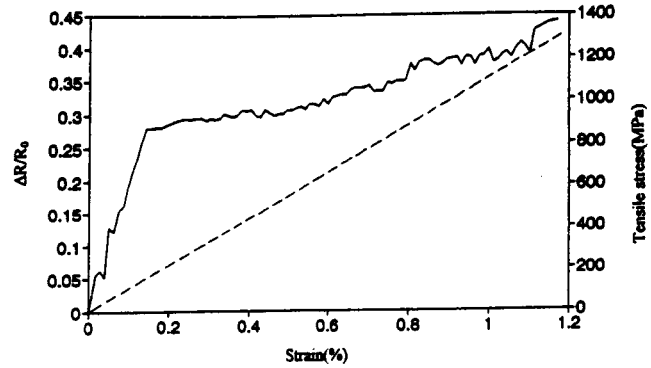

FIG. 11. Longitudinal stress and strain and the through-thickness $\Delta R/R_0$ obtained simultaneously during static tension up to fracture, which occurs at the highest strain in the curves, for continuous carbon fiber epoxy-matrix composite. Solid curve: $\Delta R/R_0$ versus strain. Dashed curve: tensile stress versus strain.

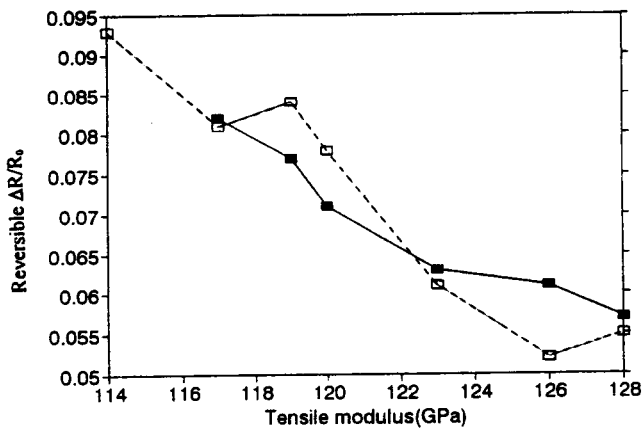

FIG. 12. Variation of the absolute value of the reversible part of $\Delta R/R_0$ with the longitudinal tensile modulus for continuous carbon fiber epoxy-matrix composite. Solid curve and solid rectangles: longitudinal $\Delta R/R_0$, obtained at a fixed stress amplitude equal to 35% of the breaking stress. Dashed curve and open rectangles: through-thickness $\Delta R/R_0$, obtained at a fixed stress amplitude equal to 30% of the breaking stress.

totally reversible (Figs. 8 and 10), when the strain is reversible. That the reversible part of $\Delta R/R_0$ is due to the decrease in the degree of marcelling upon longitudinal tension is supported by the fact that the longitudinal tensile modulus decreases with increasing magnitude of the reversible part of $\Delta R/R_0$ (Fig. 12) and that the longitudinal tensile modulus is known to decrease with increasing degree of marcelling. In other words, the higher the degree of marcelling under no load, the greater the magnitude of the reversible part of $\Delta R/R_0$. Also consistent with the notion that the reversible part of $\Delta R/R_0$ is due to the decrease in the degree of marcelling upon longitudinal tension is the observation that the absolute value of the reversible part of the longitudinal $\Delta R/R_0$ increases with increasing longitudinal resistivity at no load (Fig. 13), and that the reversible part of transverse $\Delta R/R_0$ decreases

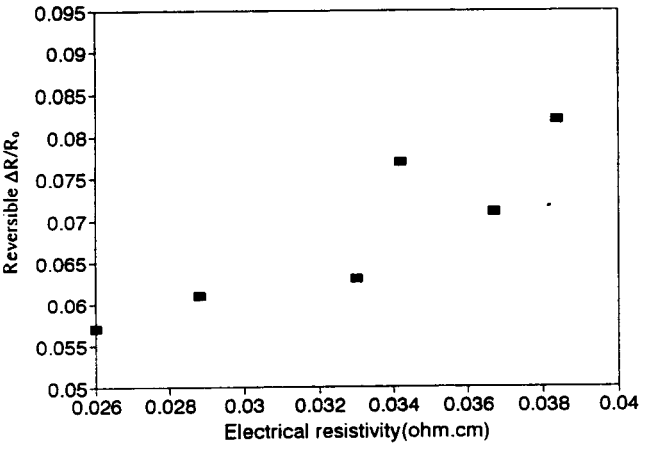

FIG. 13. Variation of the absolute value of the reversible part of the longitudinal $\Delta R/R_0$ with the longitudinal resistivity at no load for continuous carbon fiber epoxy-matrix composite.

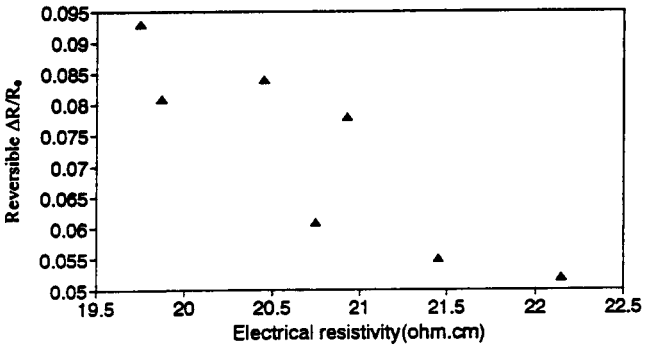

FIG. 14. Variation of the reversible part of the through-thickness $\Delta R/R_0$ with the through-thickness resistivity at no load for continuous carbon fiber epoxy-matrix composite.

with increasing through-thickness resistivity at no load (Fig. 14), since the longitudinal resistivity is expected to decrease with decreasing degree of marcelling while the through-thickness resistivity is expected to increase with decreasing degree of marcelling.

The irreversible behavior, though small compared to the reversible behavior, is such that R (longitudinal or through-thickness) is irreversibly decreased after the first cycle. This behavior is tentatively attributed to the irreversible disturbance to the fiber arrangement at the end of the first cycle, such that the fiber arrangement becomes less neat. A less neat fiber arrangement means more chance for the adjacent fiber layers to touch one another.

The stepwise increase of the longitudinal $\Delta R/R_0$ in the large strain regime (Fig. 9) is attributed to fiber breakage, which probably occurs in spurts. Such a stepwise increase had been previously observed and also attributed to fiber breakage.[23]

The through-thickness $\Delta R/R_0$ increases abruptly at low strains but increases gradually at high strains (Fig. 11). This is because only a small change in the degree of marcelling causes a large change in the chance of adjacent fiber layers to touch one another, and the resistance changes abruptly with the separation between adjacent fiber layers at small separations but changes gradually with the separation at large separations. Moreover, fiber breakage, which occurs at high strains, essentially does not affect through-thickness $\Delta R/R_0$ (Fig. 11), but affects longitudinal $\Delta R/R_0$ (Fig. 9).

D. Summary

An electromechanical effect observed in unidirectional continuous carbon fiber reinforced epoxy allows the composite to serve as a sensor of its own degree of marcelling. The effect is such that the longitudinal $\Delta R/R_0$ decreases and the through-thickness $\Delta R/R_0$ increases upon longitudinal tension due to the decrease in the degree of marcelling. The strain sensitivity (gage factor) is large in magnitude (from 34 to 49). The effect is almost totally reversible when the longitudinal strain is reversible. The irreversible behavior involves $\Delta R/R_0$ (longitudinal or through-thickness), decreasing irreversibly after the first cycle due to irreversible decrease in the degree of neatness of the fiber arrangement.

The technique of this section is limited to matrices that are much less conducting than the fibers.

V. CONCLUSION

Electromechanical testing involving simultaneous electrical and mechanical measurements under load was found to be valuable for studying the fiber-matrix interface, the fiber residual compressive stress in the fiber direction, and the degree of marcelling in carbon fiber composites. The fiber-matrix interface study involves measuring the fiber-matrix contact electrical resistivity during single fiber pull-out testing. It provides information on the bond strength and the interfacial structure and allows even a small change in bond strength due to a change in interfacial structure to be observed. The fiber residual stress study involves measuring the electrical resistance of a single fiber embedded in the matrix while the fiber is subjected to tension through its two exposed ends. The tensile stress needed to decrease the resistance to a minimum value is taken to be the residual stress. The fiber marcelling study involves measuring the electrical resistance of a continuous fiber laminate in the through-thickness direction while the laminate is subjected to tension (within the elastic regime) in the fiber direction. The greater is the fractional increase in the through-thickness resistance per unit strain in the fiber direction, the higher is the degree of marcelling.

Although carbon fibers were used in all the illustrations in this paper, all techniques described in this

paper can be applied equally well to other electrically conducting fibers, such as steel fibers.

ACKNOWLEDGMENT

This work was supported in part by National Science Foundation.

REFERENCES

1. S.A. Jawad, M. Ahmad, Y. Ramadin, A. Zihlif, A. Paesano, E. Martuscelli, and G. Ragosta, Polymer Int. **32** (1), 23 (1993).
2. H.M. Hsiao and I.M. Daniel, Composites A **27** (10), 931 (1996).
3. X. Fu and D.D.L. Chung, Composite Interfaces **4** (4), 197 (1997).
4. P. Chen and D.D.L. Chung, Composites: Part B **27B**, 269 (1996).
5. P. Chen and D.D.L. Chung, Composites: Part B **27B**, 11 (1996).
6. X. Fu and D.D.L. Chung, Cem. Concr. Res. **26** (1), 15 (1996).
7. P. Chen and D.D.L. Chung, ACI Mater. J. **93** (2), 129 (1996).
8. ACI SP-142, *Fiber Reinforced Concrete,* edited by James I. Daniel and Surendra P. Shah, ACI, Detroit (1994).
9. D.J. Hannant, Mater. Sci. Technol. **11**, 853 (1995).
10. N. Banthia, A. Moncef, K. Chokri, and J. Sheng, Can. J. Civ. Eng. **21**, 999 (1994).
11. Isabel Padron and Ronald F. Zollo, ACI Mater. J. **87**, 327 (1990).
12. F. Hoecker and J. Karger-Kocsis, J. Appl. Polym. Sci. **59**, 139 (1996).
13. Hung-Lung Chiang, P.C. Chiang, and J.H. You, Toxicological Environ. Chem. **47** (1–2), 97 (1995).
14. G. Krekel, K.J. Hüttinger, W.P. Hoffman, and D.S. Silver, J. Mater. Sci. **29**, 2968 (1994).
15. X. Fu and D.D.L. Chung, Cem. Concr. Res. **27** (12), 1805 (1997).
16. X. Fu and D.D.L. Chung, Cem. Concr. Res. **26** (10), 1485 (1996).
17. A.S. Crasto and R.Y. Kim, Proc. Am. Soc. Composites, 8th Tech. Conf. (Technomic Pub. Co., Lancaster, PA, 1994), pp. 162–173.
18. C.F. Fan and S.L. Hsu, J. Polym. Sci.: Part B **27** (2), 337 (1989).
19. D.T. Grubb and Z. Li, J. Mater. Sci. **29** (1), 203 (1994).
20. K.S. Kim and H.T. Hahn, Composites Sci. Technol. **36** (2), 121 (1989).
21. X. Wang and D.D.L. Chung, Carbon **35** (5), 706 (1997).
22. R.S. Feltman and M.H. Santare, Composites Manuf. **5** (4), 203 (1994).
23. K. Schulte and Ch. Baron, Composites Sci. Technol. **36**, 63 (1989).